GUIDANCE AND CONTROL OF AFFORDABLE GUIDED AIRDROP SYSTEM

O.Yakimenko, V.Dobrokhodov, J.Johnson, I.Kaminer
Naval Postgraduate School, Monterey, CA

S.Delliker
U.S. Army Yuma Proving Ground, Yuma, AZ

R.Benney
U.S. Army Soldier and Biological Chemical Command, Natick, MA

Abstract: This paper addresses the development of an autonomous guidance, navigation and control system for a flat solid circular parachute. This effort is a part of the Affordable Guided Airdrop System (AGAS) that integrates a low-cost guidance and control system into fielded cargo air delivery systems. The paper describes the AGAS concept, its architecture and components. It further proceeds with the description of the control strategy based on Pontrjagin's principle of optimality. The paper ends with the results of the final AGAS demonstration performed at the U.S. Army Yuma Proving Ground in September, 2001. *Copyright © 2002 by IFAC.*

Keywords: automated guided vehicles, optimal control, flight control

I. INTRODUCTION

As identified in the Summary Report: New World Vistas, Air and Space Power for the 21st Century," *United States Air Force Science Advisory Board*, 1997 there is an urgent need to improve the point-of-use delivery; that is, getting the materiel where it needs to be, when it needs to be there. This statement served as an initial point for the Affordable Guided Airdrop System (AGAS) project, initiated by the U.S. Army in mid 90s, see (Brown, at al., 1999).

Currently, high-altitude, low-opening and high altitude, high-opening airdropped personnel are the only assets that can be released from altitudes above 1500m while still realizing an acceptable landing accuracy. Aerial missions over Bosnia in 1993 underscored high-altitude airdropped payload delivery accuracy concerns during operations conducted from above 3000m for re-supply and humanitarian purposes (over 50% of all cargo ended up at the wrong spots). Humanitarian-relief airdrops over Kosovo in 1999 and Afganistan in 2001 demanded that airdrop aircraft operate from even higher altitudes, with an expected further degradation of payload delivery accuracy.

These facts have led to the main design goal of the AGAS development - to provide Guidance, Navigation, and Control (GNC) system that can be placed in-line with existing fielded cargo parachute systems (G-12 and G-11) and standard delivery containers (A-22). The system was required to provide an accuracy of at least 100m with a desired goal of 50m. No changes to the parachute or cargo system were allowed.

The key ideas of AGAS concept can be easily understood from the following.

The first step is for the user to broadcast a supply request that includes information on where and when it is needed on the ground. Upon arrival at the assigned drop zone (DZ) the delivery aircraft drops a wind dropsonde. The wind profile acquired during this drop allows computation of the reference trajectory (RT) and of the Computed Air Release Point (CARP). The aircraft will then be navigated to that point for air delivery of the materiel (payload). Should the wind estimate and calculation of CARP be perfect and the aircrew gets the aircraft to this point precisely, then the parachute would fly along RT towards the TA with no control inputs required. However, wind estimation is not a precise science. Furthermore, calculation of the CARP relies on less than perfect estimates of parachute aerodynamics and the flight crews cannot precisely hit CARP for each airdrop mission (especially in case of massive (multiple) deliveries). Therefore, the AGAS GNC system is used to overcome these potential errors.

AGAS design concept employs commercial Global Positioning System (GPS) receiver and a heading reference as navigation sensors, an inexpensive guidance computer to determine and activate the desired control inputs, and application of Pneumatic Muscle Actuators (PMAs) to generate control inputs. The navigation system and guidance computer are secured to existing container delivery system, while PMAs are attached to each of four parachute risers and to the container. Control is affected by lengthening one or two adjacent risers. Upon deployment of the system from the aircraft, the guidance computer steers the system along pre-planned RT. The AGAS concept relies on the sufficient control authority to be produced to overcome errors in wind estimation and the point of release of the system from the aircraft.

Present paper gives an overall view of the development of GNC algorithms for the AGAS project starting with the classical synthesis of an optimal control using Pontrjagin's Maximum Principle (Section II), followed by description of the practical algorithm implemented in simulations and flight test (Section III). Finally Section IV shows the setup and results of a final flight test performed at the YPG in September 2001, see (PATCAD, 2001).

II. SYNTHESIS OF CONTROL ALGORITHMS

Based on the AGAS concept introduced above, the optimal control problem for determination of parachute trajectories from an actual release point (RP) to TA can be formulated as follows: *among all admissible trajectories that satisfy the system of differential equations, given initial and final conditions and constraints on control inputs, determine the optimal trajectory that minimizes a cost function of state variables $\bar{z}$ and control inputs $\bar{u}$*

$$J = \int_{t_0}^{t_f} f_0(t, \bar{z}, \bar{u}) dt \qquad (1)$$

and compute the corresponding optimal control.

For the AGAS, the most suitable cost function J is the number of PMA activations. Unfortunately this cost function cannot be formulated analytically in the form given by expression (1). Therefore, we investigated other well-known integrable cost functions and used the results obtained to determine the most suitable cost function for the problem at hand.

To determine the optimal control strategy we applied Pontrjagin's principle to a simplified kinematic planar (3-DoF) model of parachute, see (Pontrjagin, et al., 1969). Two possible control schemes are considered in the following subsections. The first one applies directly to the control problem at hand, while the second addresses a possible future control configuration. In each case we consider a no wind scenario. Therefore, the control objective is to steer the parachute to a single stationary point onto a horizontal plane. This is a reasonable approximation of since the control inputs have a negligible effect on the descent rate.

II.1. Symmetric control

The simplest model describing parachute kinematics in the horizontal plane with four equal on-off controllers may be written as follows (Fig.1):

$$\dot{x} = \begin{pmatrix} u & v \end{pmatrix} \begin{pmatrix} \cos \psi \\ -\sin \psi \end{pmatrix}, \ \dot{y} = \begin{pmatrix} u & v \end{pmatrix} \begin{pmatrix} \sin \psi \\ \cos \psi \end{pmatrix}, \ \dot{\psi} = const . \quad (2)$$

This model approximates the impact on the parachute velocity in the lateral plane caused by the activation of each of the four PMAs: $u, v \in [-V; 0; V]$. We consider these speed components as controls for the task at hand.

The Hamiltonian for the system (2) can be written in the following form:

$$H = \begin{pmatrix} u, v \end{pmatrix} \begin{pmatrix} p_x \cos \psi + p_y \sin \psi \\ -p_x \sin \psi + p_y \cos \psi \end{pmatrix} + p_\psi const - f_0, \quad (3)$$

where differential equations for the adjoint variables p_x, p_y, and p_ψ are given by

$$\dot{p}_x = 0, \quad \dot{p}_y = 0, \quad \dot{p}_\psi = \begin{pmatrix} p_x, p_y \end{pmatrix} \begin{pmatrix} u \sin \psi + v \cos \psi \\ -u \cos \psi + v \sin \psi \end{pmatrix}. \quad (4)$$
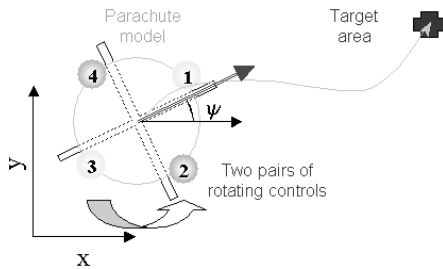

Fig.1. Projection of the optimization task onto the horizontal plane.

We consider two cost functionals

$$f_0 \equiv 1 \ \text{and} \ f_0 \equiv |u| + |v| \quad (5)$$

usually being used for the minimum-time and minimum fuel problems. Note that in this particular application the second cost function stands for the momentum or energy rather than fuel since AGAS spends gas only to activate

PMAs (there is no gas expenditure needed to maintain PMA filled/vented).

Note also that in principle we are looking at the optimal problem with a fixed time (time of descent). However in real life under the actions of atmospheric turbulence and disturbances it would be a good idea to steer parachute to the TA as soon as possible leaving some extra time to fight those disturbances for the rest of the drop.

According to Pontrjagin's principle, the optimal control is determined as $\vec{u}_{opt} = argmax H(\vec{p}, \vec{z}, \vec{u})$. Therefore, for the time-minimum problem the optimal control is given by

$$u = V sign \left(\begin{pmatrix} p_x, p_y \end{pmatrix} \begin{pmatrix} \cos \psi \\ \sin \psi \end{pmatrix} \right), \ v = V sign \left(\begin{pmatrix} p_x, p_y \end{pmatrix} \begin{pmatrix} -\sin \psi \\ \cos \psi \end{pmatrix} \right). \quad (6)$$

Fig.2 shows the graphical interpretation of these expressions. In general, the vector $\begin{pmatrix} p_x, p_y \end{pmatrix}$ defines a direction towards the TA and establishes a semi-plane perpendicular to itself that defines the nature of control actions. Specifically, if PMA happens to lie within a certain operating angle (OA) Δ with respect to the vector $\begin{pmatrix} p_x, p_y \end{pmatrix}$ it should be activated. For a time-optimum problem $\Delta = \pi$ - therefore, two PMAs will always be active. Parachute rotation determines which two. (We do not address the case of singular control, which in general is possible if the parachute is required to satisfy a final condition for heading.)
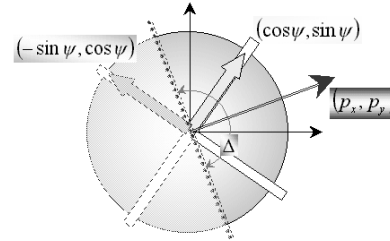

Fig.2. Time-optimal control.

Fig.3 shows an example of time-optimal trajectory. It consists of several arcs and a sequence of actuations. For the sake of simplicity $\dot{\psi} = 2°/s$ was taken for this simulation (as observed in one of the earlier flight-tests).[1] Maximum horizontal velocity of $V=3.7m/s$ was used in this example.

For the 'fuel'-minimum problem we obtain analogous expressions for the optimal control inputs:

$$
\begin{aligned}
p_x \cos \psi + p_y \sin \psi > V &\Rightarrow u = V, \\
p_x \cos \psi + p_y \sin \psi < V &\Rightarrow u = -V, \\
p_x \cos \psi + p_y \sin \psi \equiv V &\Rightarrow u = u_{s.c.}; \\
-p_x \sin \psi + p_y \cos \psi > V &\Rightarrow v = V, \\
-p_x \sin \psi + p_y \cos \psi < V &\Rightarrow v = -V, \\
-p_x \sin \psi + p_y \cos \psi \equiv V &\Rightarrow v = v_{s.c.}.
\end{aligned} \quad (7)
$$

In this case PMAs will be employed when an appropriate dot product is greater than some positive value. Obviously, this narrows the OA's magnitude. In fact, for this particular cost function $\Delta \to 0$ [2]. In general any cost function other

---

[1] In principle because of symmetry no rotation should be observed unless any kind of asymmetry is introduced.

[2] Note that any control with $\Delta < 0.5\pi$ may not work at all if parachute is not rotating.

than minimum-time will require an operating angle $\Delta \le \pi$ (Fig.4).
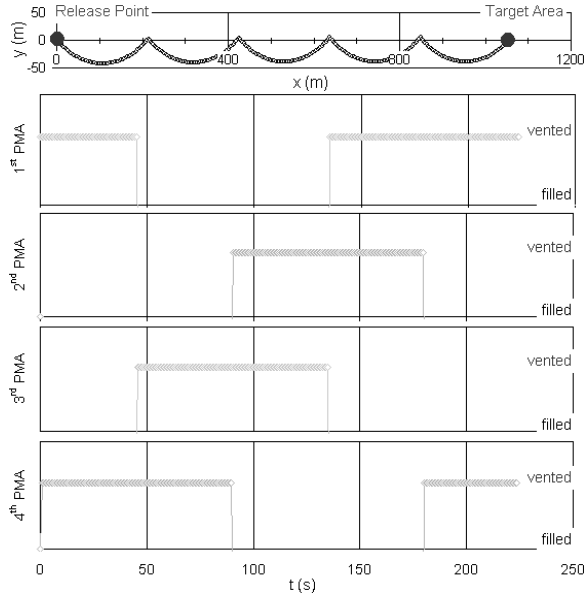

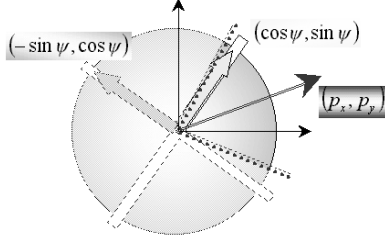Fig.3. Example of the time-optimal trajectory and time-optimal controls.

Fig.4. Generalized case of optimal control.

Fig.5 shows the effect of OA's magnitude on the flight time, 'fuel' and number of PMA activations (from 'vented' to 'filled' state). It is clearly seen that the nature of the dependence of the number of actuations on OA is the same as that of the time of flight. This implies that by solving the time-minimum problem we automatically ensure a minimum number of actuations. Moreover, it is also seen that the slope of these two curves in the interval $\Delta \in [0.5\pi; \pi]$ is flat. This implies that small changes of OA from its optimal value will result in negligible impact on the number of actuations. Therefore, changing the OA to account for the realistic PMA model, as is done on AGAS, will not change the number of actuations significantly.

Fig.6 demonstrates the influence of constant yaw rate on different OA's. The results were obtained for the time optimal control problem illustrated in Fig.3. Obviously, the smaller the yaw rate is, the smaller the number of activations. Decreasing OA for the same yaw rate leads to an increase in the number of PMA activations.

Fig.7 includes simulation results for the case where yaw angle from a flight test was used to drive the first two equations in (2) while optimal control was computed using (6). As can be seen the flight test heading is not smooth. Neither is it monotonic. Although a synthesized optimal control drives the model of the parachute towards TA, because of the erratic yaw the number of PMA actuations increases to 35 (versus 12 with the monotonic 2 %/s yaw rate as seen from Fig.5). For this particular simulation OA was equal to 2.5. This example illustrates sensitivity of the optimal control algorithm to uncertainties in heading. Therefore, flight control algorithm must be more robust to

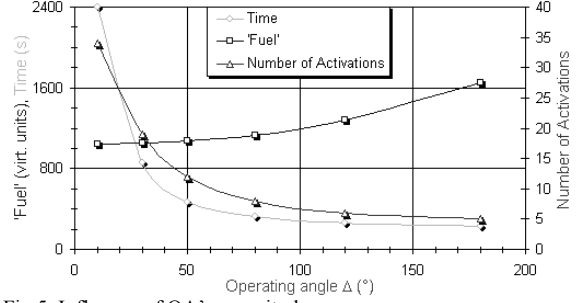these uncertainties to prevent a significant increase in the number of PMA actuations.
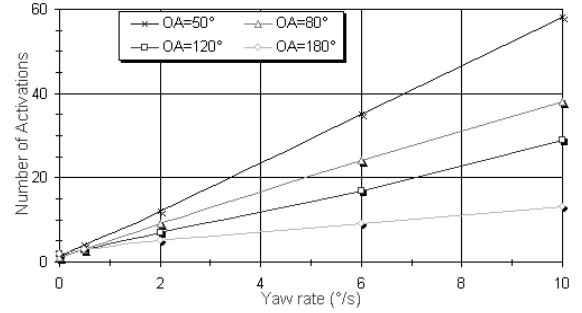

Fig.5. Influence of OA's magnitude.

Fig.6. Influence of a constant yaw rate.

II.2. Asymmetric control

We now consider another kinematic model of a parachute in the horizontal plane with the different control architecture. Suppose that after initial deployment and filling of all four PMAs one of them is vented and remains vented throughout the drop. This provides a constant glide ratio (similar to parafoils). Furthermore, suppose that two adjacent PMAs can be half-filled (that means their length could be set as an average between filled and full-vented states). The resulting artificially introduced asymmetry allows us to control parachute's yaw rate. Mathematically, this is expressed by the following simplified equations:

$$\dot{x} = V \cos\psi\, , \quad \dot{y} = V \sin\psi\, , \quad \dot{\psi} = v + \zeta(t)\, , \qquad (8)$$

where $v \in [-\Xi; 0; \Xi]$ is now the only control (in practice for G-12 based AGAS Ξ would be equal to about 6 %/s).

The Hamiltonian for the system (8) can now be written as:

$$H = p_\psi v + V\left(p_x, p_y\right)\begin{pmatrix}\cos\psi \\ \sin\psi\end{pmatrix} + p_\psi \zeta(t) - f_0\, , \qquad (9)$$

where equations for adjoint variables p_x, p_y and p_ψ are given by

$$\dot{p}_x = 0, \quad \dot{p}_y = 0, \quad \dot{p}_\psi = V\left(p_x, p_y\right)\begin{pmatrix}\sin\psi \\ -\cos\psi\end{pmatrix}. \qquad (10)$$

The optimal control for the time-minimum problem now is given by

$$v = \Xi\, sign\left(p_\psi\right). \qquad (11)$$

By differentiating last expression in (10) and combining it with Hamiltonian (9) for both cases when $p_\psi > 0$ and $p_\psi < 0$ we can get a set of equations for p_ψ

$$\ddot{p}_\psi + \Xi^2 p_\psi \mp \Xi = 0 \qquad (12)$$

giving two sinusoids (shifted with respect to abscise axis by $\pm\Xi^{-1}$) as solutions for the general (non-singular) case

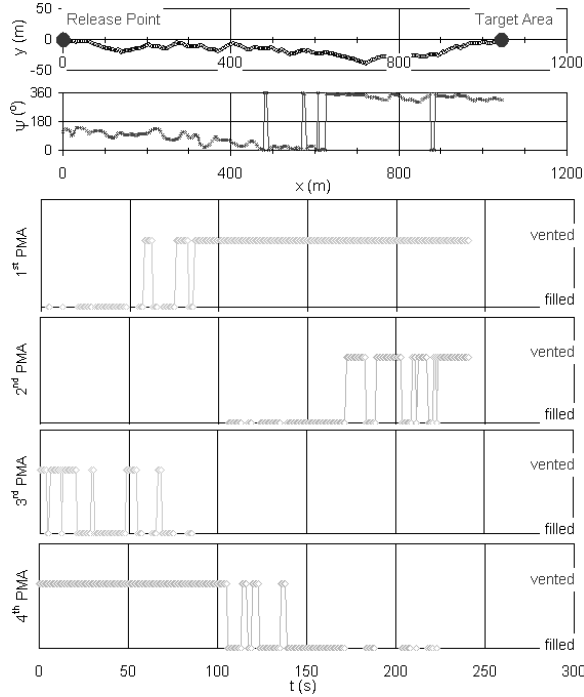$$p_\psi = C_1 \sin(\Xi t + C_2) \pm \Xi^{-1} . \qquad (13)$$

Fig.7. Flight path computed with usage of a real heading profile.

If $C_1 \neq \Xi^{-1}$ the parachute model moves along a descending spiral. It takes $2\pi\Xi^{-1}$ seconds to make a full turn with a radius of $V\Xi^{-1}$ (that gives $\sim60s$ and $\sim40m$ in case of 'modified' AGAS respectively). If $C_1 = \Xi^{-1}$ there exists a possibility of singular control. This is caused by the fact that there exists a point in time where both p_ψ and $\dot{p}_\psi$ are zero as can be seen in (13).

Consider singular control for this model. By definition it means that $p_\psi \equiv 0$. For the time-optimal problem from the Hamiltonian (9) and third equation in (10) (of course keeping in mind the first two) it follows that for a singular control case

$$p_x = V^{-1}\cos\psi , \quad p_y = V^{-1}\sin\psi , \quad \psi = const , \qquad (14)$$

Expressions (14) imply that singular control corresponds to motion with constant heading ($v \equiv 0$). It may not however be realized. Instead, the parachute model may switch from right-handed spiral to a left-handed one or vice versa. Planar projections of possible trajectories are shown on Fig.8.
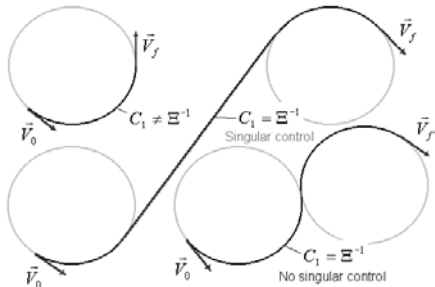

Fig.8. Possible types of AGAS trajectories in case of potential asymmetric control.

The time-optimal trajectories for this case are shown in Fig.9 (trajectories differ by initial orientation of the model). The only PMA actuation is needed in this case to turn parachute velocity vector towards TA at the start.

To conclude this subsection it worth noting that control algorithms for parafoils (since their control options are quite similar to the discussed above) suggest the same logic consisting of spiral motion in the beginning immediately after deployment followed straight-line gliding towards TA.

III. FLIGHT CONTROL ALGORITHM

The actuation box for PMA's developed by Vertigo is capable of only bang-bang control. Optimal control analysis of a simplified parachute model discussed in Section II suggested that bang-bang is also the optimal control strategy and produced an important concept of an operating angle. This motivated the following basic control concept for AGAS. Since the time-optimal control strategy was shown to minimize the number of actuations for a planar model this strategy was employed to get the parachute to within a predefined altitude-dependent TA (defined by inner and outer cones discussed next) and then for the remainder of descent to stay within this area. In addition, this basic strategy must be robust to uncertainties in yaw motion. These considerations were used to develop the flight control algorithm for AGAS and are detailed next.

III.1. Basic control architecture

Considering the relatively low glide ratio demonstrated in flight test AGAS can only overcome less than $4m/s$ wind. It is therefore imperative that the control system steers the parachute along a pre-specified RT obtained from most recent wind prediction. This can be done by comparing the current GPS position of the parachute with the desired one on RT at a given altitude to obtain the position error

$$\vec{P}_e(h) = \vec{P}_{AGAS}(h) - \vec{P}_{CARP}(h) . \qquad (15)$$

This position error $\vec{P}_e(h)$ is computed in inertial (LTP) coordinate system with an origin in the TA and is then converted to the body axis using an Euler angle rotation $_I^B R$ (computed using yaw angle only). The resulting body-axis error vector

$$\vec{P}_B = {}_I^B R(\vec{P}_e) \qquad (16)$$

is then used to identify error angle (EA)

$$EA = \arg\vec{P}_B . \qquad (17)$$

In turn EA is then used to define what PMA ($i = 1,...,4$) must be activated:

$$i = \begin{cases} 1, & if \quad EA \leq \dfrac{\Delta}{2} \vee EA \geq 2\pi - \dfrac{\Delta}{2}, \\ 2, & if \quad EA \in \left[\dfrac{3\pi}{2} - \dfrac{\Delta}{2}; \dfrac{3\pi}{2} + \dfrac{\Delta}{2}\right], \\ 3, & if \quad EA \in \left[\pi - \dfrac{\Delta}{2}; \pi + \dfrac{\Delta}{2}\right], \\ 4, & if \quad EA \in \left[\dfrac{\pi}{2} - \dfrac{\Delta}{2}; \dfrac{\pi}{2} + \dfrac{\Delta}{2}\right] \end{cases} \qquad (18)$$

(by definition EA is counted from PMA #3 counterclockwise, i.e. in the situation shown as example on Fig.10 PMAs #2 and #3 would be activated (vented).
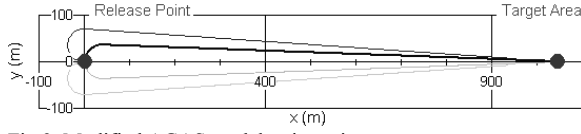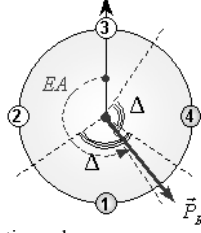
Fig.9. Modified AGAS model trajectories.

Fig.10. Control-activation rule.

In order to account for the refill time and sensors errors the operating angle was set to $\Delta \approx 2.5$ instead of $\Delta = \pi$ [3]. This still allows the activation of a single control input or two simultaneous control inputs without significant degradation of AGAS performance (see Fig.5).

III.2. Outer and inner cones

First of all the initial error after deployment should not exceed a certain value because of AGAS' limited control authority. This area of attraction has the radius R_A around RT that can be roughly estimated by a simple formula

$$R_A(h) = 0.8 k_\Delta GR_{\max} h \text{ , where } k_\Delta \approx \Delta \pi^{-1}. \qquad (19)$$

Coefficient k_Δ is approximated by using the data of Fig.5, and coefficient 0.8 accounts for real-world yaw profile.

To eliminate unnecessary actuations of PMAs a tolerance (outer) cone was established. Its radius at CARP (at an altitude of $3000m$) is $\Re_{outer}(3000) = 200m$ and decreases linearly to $\Re_{outer}(0) = 100m$ at the TA (at ground level). Should the magnitude of the position error in the lateral plane $\left| \vec{P}_B(h) \right|$ be outside of this tolerance cone

$$\left| \vec{P}_B(h) \right| > \Re_{outer}(h), \qquad (20)$$

a control is activated to steer the system back to the planned RT.

When the system is within the inner cone $\Re_{inner}$

$$\left| \vec{P}_B(h) \right| < \Re_{inner}, \qquad (21)$$

(which is set to $60m$-radius regardless of altitude) the control is disabled and the parachute drifts with the wind ($\Re_{inner}$ was selected to account for the refill time) until outer cone is reached and control is activated again.

The basic control strategy uses the following **activation rule**: both the tolerance cone and the operating angle constraints must be active for a given PMA to be actuated.

III.3. Robustness issues

The control algorithm outlined above was flight tested at YPG. As expected the number of PMA actuations was unacceptably high. This resulted in a premature emptying

---

[3] On the earliest AGAS versions refill time was not constant and was equal to about $20s$ at the end, that for the yaw rate of $2 °/s$ gives around $40°$.

of PCS tanks. Analysis of flight test data indicated that this was caused by frequent heading changes and that that these changes occurred when one of the adjacent PMAs was actuated while the other one was in transition from vent to full or vice versa.

Fig.11 explains this phenomenon. If one PMA is activated (vented) and adjacent PMA is performing a transition from one state to another this causes a yaw moment $\vec{M}_c$. This moment can be 'useful' (when the direction of rotation of the vector $\vec{P}_B$ is opposite to the direction of $\vec{M}_c$), or harmful (vise versa). In the latter case the rotation of the parachute under the action of $\vec{M}_c$ causes a deactivation command to the PMA that was just activated. Moreover during this deactivation the 'useful' moment in turn makes situation even worse. This case is shown on Fig.12a.
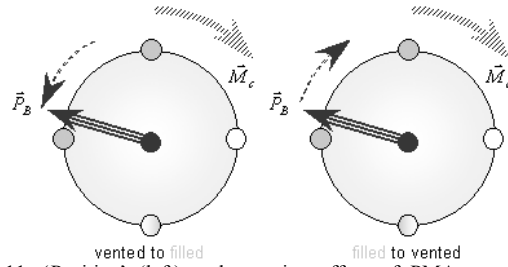

Fig.11. 'Positive' (left) and negative effect of PMA transition moment.

To eliminate unnecessary activations a delay logic in each PMA channel was introduced. Any new command that requires change in the PMA state triggers the delay timer. While the delay timer is active no command is executed including the triggering command. At the end of the delay the timer is reset and the first available command is executed until the next command that requires change in the PMA state triggers the delay timer again.

The number of unnecessary actuations can also be reduced by introducing hysteresis as shown on Fig.12c.
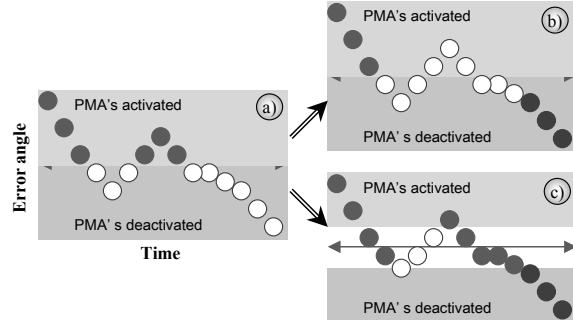

Fig.12. Two ways of decreasing the influence of yaw oscillations.

Both delay and hysteresis angle values can be adjusted as a function of system dynamics and in principle achieve the same result.

Finally, Fig.13 summarizes the previous discussion and shows the decrease of total number of PMA activations when more sophisticated control logic is employed.

IV. FLIGHT TEST

A total of about 15 controlled drops were made at YPG to test the AGAS concept. The final demonstration took place at YPG during Precision Airdrop Technology Conference and Demonstration (PARCAD) on September 13th and 14th 2001.

During preliminary tests a ground station was used to control AGAS via a wireless modem. The AGAS sent its current position and heading to the ground station, the ground station processed the data using the flight control algorithm and then issued appropriate commands to the AGAS GNC.
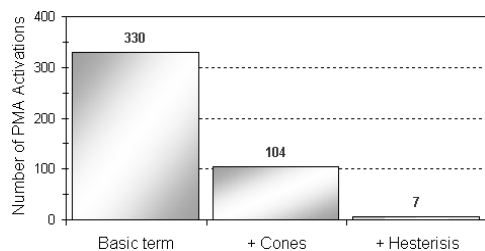

Fig.13. Number of PMAs activations decrease.

For the final drops all GNC algorithms were executed aboard AGAS. The downlink message was used real-time monitoring during the drop.

The rest of the paper describes a pre-flight procedure, flight test setup and the results of two successful drops of four AGAS performed during final Precision Airdrop Technology Conference and Demonstration (PATCAD) demonstration.

IV.1. Flight test setup

According to the general procedure after AGAS had been rigged, pressurized, and charged, it was taken to the scales to be weighed, and a communication link check was also performed. Next, the system was loaded onto the aircraft and the main valve was opened.

When the aircraft was at a drop altitude and before it started its cold pass over the DZ, the main power switch was turned on and the GNC hardware was armed. As the plane arrived at the CARP, the AGAS system was deployed, as well as a door-deployed wind-pack bundle that was weighted to descend at the same rate as the AGAS system (to provide real wind profile during the drop for the future analysis).

Fig.14 shows the sequence of deployment during PATCAD demonstration. To make the difference between non-controlled and controlled parachute more clear two standard G-12 and two AGAS (followed by the wind-pack) were deployed simultaneously.
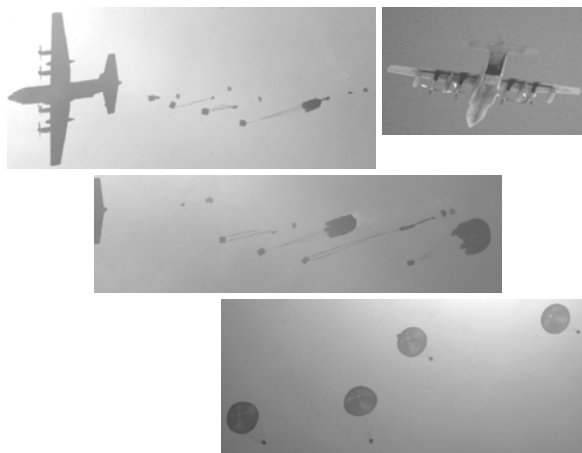

Fig.14. Deployment sequence.

IV.2. Flight data analysis

Several same-weight category systems including both circular parachutes and parafoils were demonstrated at PATCAD. AGAS performed better than others. The miss for the four AGAS systems released was less than 78m as oppose to 140-1370m for uncontrolled parachutes (see Table 1[4]).

Table 1. PATCAD results.

Date	Test Item	Weight *(kg)*	IP miss *(m)*
Sept. 13th	*WindPack*	21	515.1
	STD G-12	724	512.2
	STD G-12	773	141.9
	AGAS-1	**726**	**76**
	AGAS-2	**726**	**78**
Sept. 14th	*WindPack*	21	1048.6
	STD G-12	726	1371.6
	AGAS-3	**726**	**347.3**
	AGAS-4	**726**	**55.5**

Fig.15 demonstrates the integral data for two first-day drops from the altitude of 3000m. The 30-*minute* old wind data was used to compute the RT. It is seen that regardless a large initial error both AGAS steered to the TA fairly well, 17 and 18 PMA activations were needed to hit the target with approximately the same miss distance.
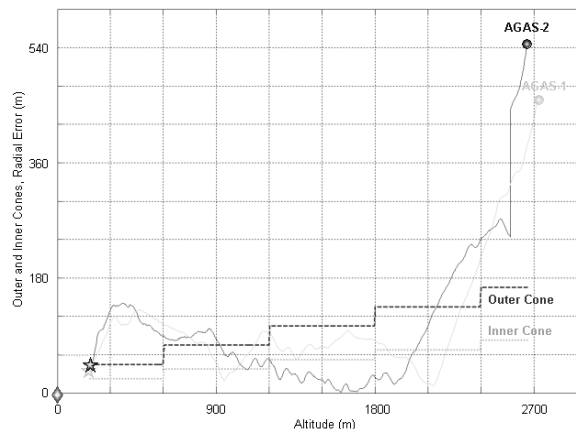

Fig.15. September 13th 3000m drops.

V. CONCLUSIONS

Results presented in this paper showed feasibility of the AGAS concept. A bang-bang control strategy imposed by the PMA hardware was developed to successfully drive AGAS to TA within prescribed circular error in flight tests at YPG. The key to the success of this strategy were concepts of operating angle motivated by optimal control analysis as well as inner and outer cones and hysteresis included to improve performance robustness.

REFERENCES

Brown, G., Haggard, R., Almassy, R., Benney, R. and Dellicker, S. (1999). The Affordable Guided Airdrop System. In: *Proceedings of 15th CAES/AIAA Aerodynamic Decelerator Systems Technology Conference*, Toulouse, France.

PATCAD (2001). http://yuma-notes1.army.mil/mtea/patcadreg.nsf.

Pontrjagin, L., Boltjanskiy, V., Gamkrelidze, R. and Mishenko, E. (1969). *Mathematical Theory of Optimal Processes*. Nayka, Moscow.

---

[4] On September 14th AGAS-1 quit working half the way down because of valve system malfunction.